

Processive Rotaxane Systems. Studies on the Mechanism and Control of the Threading Process

Pilar Hidalgo Ramos, Ruud G. E. Coumans, Alexander B. C. Deutman,
Jan M. M. Smits, Rene de Gelder, Johannes A. A. W. Elemans,
Roeland J. M. Nolte,* and Alan E. Rowan*

*Contribution from the Institute for Molecules and Materials, Radboud Universiteit Nijmegen,
Toernooiveld 1, 6525 ED Nijmegen, The Netherlands*

Received January 8, 2007; E-mail: r.nolte@science.ru.nl; a.rowan@science.nl

Abstract: The threading behavior of a zinc analogue of a previously reported processive manganese porphyrin catalyst onto a series of polymers of different lengths is reported. It is demonstrated that the speed of the threading process is determined by the opening of the cavity of the toroidal porphyrin host, which can be tuned with the help of axial ligands that coordinate to the metal center in the porphyrin.

Introduction

Processive enzymes such as DNA polymerase III and λ -exonuclease are beautiful examples of molecular nanotechnology in nature. These enzymes are highly successful in performing their tasks because they work in a pseudorotaxane topology, in which the enzyme threads on the DNA strand and slides along the chain while performing numerous rounds of catalysis before the complex dissociates.¹ These biocatalysts have served as a source of inspiration for the development of the first synthetic processive catalytic rotaxane.² By constructing a cavity-containing porphyrin macrocycle **H₂-1** (Figure 1a),³ which after insertion of a manganese center (**Mn-1**) was threaded onto a polybutadiene polymer, it was possible to mimic the catalytic action of the natural systems. It was shown that the macrocyclic catalyst can move along this polymer thread while, in the presence of an oxygen donor, catalyzing the conversion of the polymer double bonds into the corresponding epoxide functions (Figure 1c). The “outside” of the porphyrin catalyst is blocked by a bulky axial ligand, allowing the conversion of the substrate to take place preferentially (~80%) within the cavity.^{2,4} In more recent work, the threading and dethreading process of **H₂-1** on polymers of different lengths was investigated.^{5,6} Kinetic and thermodynamic studies revealed that the barrier that has to be overcome is of entropic origin and most likely related to the stretching and unfolding of the polymer chain. After finding the end of the polymer chain, the macrocycle has to move along the chain over a certain critical length before the threading process can continue. As a consequence, the rate-limiting step is dependent on the polymer

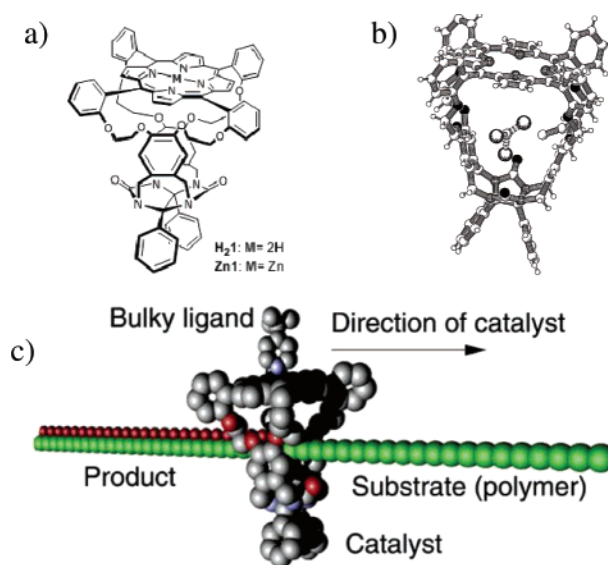


Figure 1. (a) Macrocycles **H₂-1** and **Zn-1**; (b) crystal structure of **H₂-1** (including a CHCl_3 solvent molecule); (c) schematic representation of the catalytic action of the processive catalyst.

length. This proposed mechanism is similar to the nucleation model described by Muthukumar for the translocation of a polymer through a hole.⁷ Further conclusions from the kinetic data suggested that the aforementioned processive enzyme mimic **Mn-1** most likely operates by randomly sliding along the polymer thread while performing its catalytic function. Here

- (1) Wang, J.; Sattar, A.; Wang, C. C.; Karam, J. D.; Königsberg, W. H.; Steitz, T. A. *Cell* **1997**, *89*, 1087–1099.
- (2) Thordarson, P.; Bijsterveld, E. J. A.; Rowan, A. E.; Nolte, R. J. M. *Nature* **2003**, *424*, 915–918.
- (3) Rowan, A. E.; Aarts, P. P. M.; Koutstaal, K. W. M. *Chem. Commun.* **1998**, 611–612.
- (4) Elemans, J. A. A. W.; Bijsterveld, E. J. A.; Rowan, A. E.; Nolte, R. J. M. *Chem. Commun.* **2000**, 2443–2444.
- (5) Coumans, R. G. E.; Elemans, J. A. A. W.; Rowan, A. E.; Nolte, R. J. M. *Proc. Natl. Acad. Sci. U.S.A.* **2006**, *103*, 19647–19651.

- (6) Although not related to processive catalysis, several authors have studied the threading and dethreading, and the interaction between macrocycles and polymers: (a) Mason, P. E.; Bryant, W. S.; Gibson, H. W. *Macromolecules* **1999**, *32*, 1559–1569. (b) Hodge, P.; Monvisade, P.; Owen, G. J.; Heatley, F.; Pang, Y. *New J. Chem.* **2000**, *24*, 703–709. (c) Inoue, Y.; Miyauchi, M.; Nakajima, H.; Takashima, Y.; Yamaguchi, H.; Harada, A. *J. Am. Chem. Soc.* **2006**, *128*, 8994–8995. (d) Mason, P. E.; Parsons, I. W.; Tolley, M. S. *Angew. Chem., Int. Ed. Engl.* **1996**, *35*, 2238–2241. (e) Mason, P. E.; Parsons, I. W.; Tolley, M. S. *Polymer* **1998**, *39*, 3981–3991. (f) Venturi, M.; Dumas, S.; Balzani, V.; Cao, J.; Stoddart, J. F. *New J. Chem.* **2004**, *28*, 1032–1037. (g) Wenz, G.; Gruber, C.; Keller, B.; Schilli, C.; Albusat, T.; Müller, A. *Macromolecules* **2006**, *39*, 8021–8026.

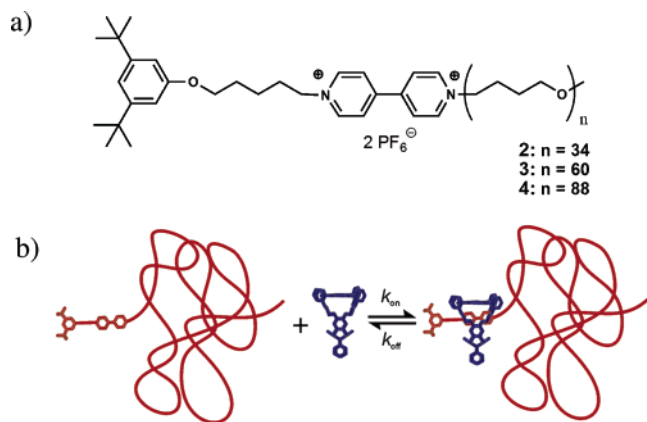


Figure 2. (a) Structure of polymers **2–4**; (b) schematic representation of the threading of host **1** on polymers **2–4**.

we describe studies on the threading behavior of **Zn-1**,⁸ an analogue of **Mn-1**, which has been designed to give more insight in the initial steps of the threading process and the role of the cavity in the motion along the thread. More specifically, we show that the initial binding of the catalyst to the polymer chain can be controlled by the addition of ligands that axially coordinate to the porphyrin metal. Coordination on the outside of **Zn-1** facilitates threading, whereas coordination on the inside of the cavity inhibits the threading process.

Results and Discussion

We recently succeeded in solving the X-ray structure of **H₂-1** (Figure 1b), which allowed us to determine the diameter of its cavity, being 8 Å. A hole of these dimensions is perfectly suited to accommodate a polymer such as polytetrahydrofuran as a thread (which has a diameter of 4.7 Å). In the current study we have employed three polytetrahydrofuran derivatives of different lengths (**2–4**),⁵ which are selectively blocked at one end by a bulky stopper group (Figure 2a). Directly linked to the blocking group, the polymers contain a viologen function (1,1'-dialkyl-4,4'-bipyridinium ion), which is known to have a high binding affinity for the cavity of **1** ($K_a = 10^6 - 10^7 \text{ M}^{-1}$).³ Consequently, the porphyrin-containing macrocycle has to completely traverse the polymer chain to reach the viologen binding site, which traps the macrocycle (Figure 2b). The complexation of **1** to the viologen trap is monitored by fluorometric techniques, that is, the porphyrin emission is quenched by the viologen once it is accommodated inside the cavity of **1**. In the case of **H₂-1**, the threading processes as followed by fluorescence quenching initially followed second-order kinetics, as plots of $1/[\text{H}_2\text{-1}]$ versus time gave straight lines. From the slope of these lines, k_{on} (rate constant for the threading process) and $\Delta G^\ddagger_{\text{on}}$ (the difference in free energy between the ground state of the uncomplexed components and the transition state) were obtained.⁵

The fluorescence curves obtained for the threading processes of **Zn-1** onto polymers **2–4** are shown in Figure 3a. Analysis of the data showed that these threading processes also follow second-order kinetics, and when the calculated k_{on} -values are compared to those found for **H₂-1**, it is evident that the

introduction of a zinc ion into the macrocyclic host leads to a much slower threading rate for each of the three polytetrahydrofuran polymers studied (Table 1). Our first impression was that this remarkable difference was caused by coordination of the zinc ion to the oxygen atoms in the polymer chains, since it is well-known that this metal center, when present in a porphyrin, prefers to bind a fifth ligand. In this way, the movement of the porphyrin macrocycle will slow down, and the average time to reach the viologen trap will increase because of the “stickiness” of the metal center to the multiple oxygen atoms of the polymer chain. However, when the $\Delta G^\ddagger_{\text{on}}$ -values for the threading of **H₂-1** and **Zn-1** where plotted versus the polymer length (Figure 3b), similar slopes were obtained ($76 \pm 21 \text{ J mol}^{-1} \text{ nm}^{-1}$ for **H₂-1** and $64 \pm 17 \text{ J mol}^{-1} \text{ nm}^{-1}$ for **Zn-1**), which indicates that the energy penalty for the macrocycle to move along the polymer thread is apparently the same for both macrocycles. The above-mentioned zinc-oxygen binding can therefore not be the major reason for the slower threading of **Zn-1**.

To obtain more insight in the threading behavior we determined the thermodynamic parameters of the process by carrying out a series of threading experiments of **Zn-1** on polymer **2** at different temperatures. From the Eyring plots, values of $\Delta H^\ddagger_{\text{on}} = 24 \pm 4 \text{ kJ mol}^{-1}$ and $\Delta S^\ddagger_{\text{on}} = -93 \pm 10 \text{ J K}^{-1} \text{ mol}^{-1}$, were calculated. When these numbers are compared to the values measured for **H₂-1** and **2** ($\Delta H^\ddagger_{\text{on}} = 20 \text{ kJ mol}^{-1}$ and $\Delta S^\ddagger_{\text{on}} = -88 \text{ J K}^{-1} \text{ mol}^{-1}$),⁵ it can be concluded that, within experimental error, the enthalpy and the entropy values of the movement along the chain are identical. We may conclude therefore that the mechanism of this motion is the same for both compounds and that **Zn-1** has no additional interactions with the thread. The difference of 6 kJ mol^{-1} in $\Delta G^\ddagger_{\text{on}}$ between **H₂-1** and **Zn-1** (Figure 3b) is apparently related to the initial threading process, which is most likely the blocking of the cavity of **Zn-1** by a molecule that has to be removed before the threading can start. Since all the threading experiments were carried out in a mixture of chloroform and acetonitrile (1:1, v/v), the latter solvent may bind to the zinc ion,⁹ preferentially on the inside of the macrocycle, acting as a competitive species for the accommodation of other guests in the cavity. If this is the case, the dimensions of the cavity are reduced to such an extent that it becomes difficult for the polymer chain to thread through the hole of **Zn-1**. To investigate if such a ligand coordination is indeed a factor that influences the threading rate, we performed several experiments in the presence of axial ligands that bind with a higher affinity to the zinc porphyrin than the acetonitrile molecule. From previous work, it was known that a 4-*tert*-butylpyridine (tbp) ligand binds to **Zn-1** on the outside of the cavity (Figure 4a). Since this binding to the outside will release the coordinated acetonitrile molecule from the inside of the macrocycle, the cavity is opened and

(9) A solution of **Zn-1** in CHCl_3 was titrated with increasing amounts of CH_3CN and the process was followed by UV–vis spectroscopy. A similar titration was carried out with zinc(II) tetrakis (2-methoxyphenyl) porphyrin and CH_3CN . From a comparison of the data it was concluded that the acetonitrile molecule binds significantly stronger to **Zn-1** than to the reference compound, suggesting strong complexation of acetonitrile inside the cavity.

(10) Using larger amounts of tbp might significantly affect the polarity of the system, causing a change in the affinity of the viologen moiety for the cavity of **1**. A blank experiment using **H₂-1** under the applied conditions, however, did not reveal any notable effect on the threading rate constant (k_{on}).

(7) Muthukumar, M. *Phys. Rev. Lett.* **2001**, *86*, 3188–3191.

(8) Elemans, J.; Claase, M. B.; Aarts, P. P. M.; Rowan, A. E.; Schenning, A.; Nolte, R. J. M. *J. Org. Chem.* **1999**, *64*, 7009–7016.

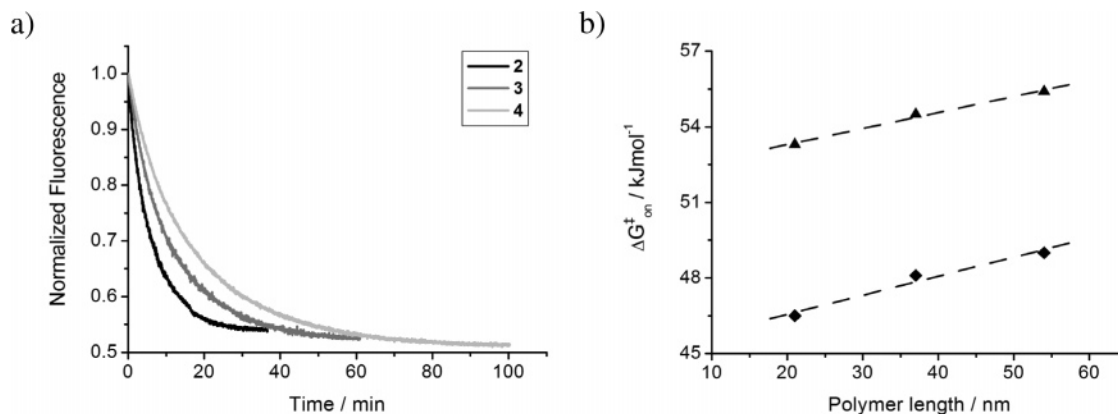


Figure 3. (a) Normalized fluorescence intensity of **Zn-1** vs time measured after the addition of 1 equiv of polymers **2–4** to the solution of this host ($[\text{Zn-1}] = [\text{2–4}] \approx 0.7 \mu\text{M}$, $\text{CHCl}_3/\text{MeCN}$ (1/1, v/v)). (b) $\Delta G_{\text{on}}^{\ddagger}$ -values for **H₂-1** (◆) and for **Zn-1** (▲) plotted vs the length of **2–4**.

Table 1. Measured k_{on} ($\text{M}^{-1} \text{s}^{-1}$) and $\Delta G_{\text{on}}^{\ddagger}$ (kJ mol^{-1}) Values for the Threading Processes Involving Macrocycles **H₂-1** and **Zn-1** and Polymers **2–4** at 296K^a

polymer	H₂-1		Zn-1		Zn-1 + tbbpy (50% bound)		Zn-1 + py (50% bound)		Zn-1 + py (99% bound)	
	k_{on}	$\Delta G_{\text{on}}^{\ddagger}$	k_{on}	$\Delta G_{\text{on}}^{\ddagger}$	k_{on}	$\Delta G_{\text{on}}^{\ddagger}$	k_{on}	$\Delta G_{\text{on}}^{\ddagger}$	k_{on}	$\Delta G_{\text{on}}^{\ddagger}$
2	36000	47	2300	53	4690	52	700	56	34	64
3	19000	48	1400	54	2560	53	560	57	21	65
4	12000	49	980	55	1990	54	325	58	12	66

^a Estimated error on $k_{\text{on}} = 30\%$.

Table 2. Calculated K_{a} (M^{-1}) for the Binding of **H₂-1** and **Zn-1** to Polymers **2–4** at 296K^a

polymer	H₂-1		Zn-1		Zn-1 + tbbpy (50% bound)		Zn-1 + py (50% bound)		Zn-1 + py (99% bound)	
	k_{on}	$\Delta G_{\text{on}}^{\ddagger}$	k_{on}	$\Delta G_{\text{on}}^{\ddagger}$	k_{on}	$\Delta G_{\text{on}}^{\ddagger}$	k_{on}	$\Delta G_{\text{on}}^{\ddagger}$	k_{on}	$\Delta G_{\text{on}}^{\ddagger}$
2	2.8×10^7	2.7×10^6	1.49×10^7	9.72×10^5	1.72×10^5					
3	2.9×10^7	2.8×10^6	7.10×10^6	1.23×10^6	1.72×10^5					
4	3.0×10^7	2.8×10^6	9.50×10^6	1.15×10^6	2.60×10^5					

^a Estimated error on $K_{\text{a}} = 50\%$.

ready to thread. Because of the rather low association constant between **Zn-1** and tbbpy ($K_{\text{a}} = 250 \text{ M}^{-1}$), ~ 6300 equiv of the ligand were used in the threading experiments to ensure an approximate 50% binding to the porphyrin.¹⁰ Upon the addition of each of the polymers **2–4** to **Zn-1** in the presence of tbbpy in a $\text{CH}_3\text{CN}/\text{CHCl}_3$ solution (1:1, v/v), a faster quenching of porphyrin fluorescence was observed (Table 1), indicating that the rate of the threading of **Zn-1** is indeed related to the release of an axially binding solvent molecule (acetonitrile) from the cavity. To obtain additional evidence for this hypothesis, the cavity of **Zn-1** was intentionally blocked by the addition of pyridine (py) to the host (Figure 4b). As a result of stabilizing π – π stacking interactions and a cavity effect, this smaller axial ligand binds very strongly within the cavity of **Zn-1** ($K_{\text{a}} = 1.1 \times 10^5 \text{ M}^{-1}$ in CDCl_3),⁸ and at low concentrations ($\sim 10^{-6} \text{ M}$) only a few equivalents are needed to achieve a nearly quantitative binding. In a first experiment, a calculated amount of pyridine was added so that on average 50% of the cavities of **Zn-1** were occupied, and upon the addition of each of the polymers this indeed resulted into a much slower threading rate (Figure 5a). Upon the addition of more equivalents of py to the system (so that $\sim 99\%$ of the cavities were occupied), the k_{on} -values dropped dramatically, and a nearly complete blocking of the threading process was achieved (Table 1). In Figure 5a, all threading experiments of **Zn-1** on polymer **2** in the presence

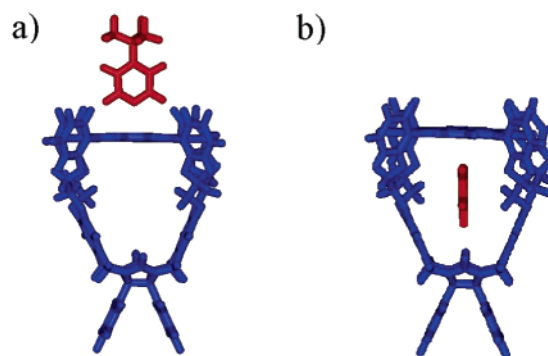


Figure 4. (a) Schematic representation of the complexation of tbbpy to the “outside” of **Zn-1**; (b) schematic representation of the cavity of **Zn-1** filled with py.

or absence of axial ligands are compiled, illustrating the clear difference in time required for the toroidal host to reach the viologen trap at the blocked end of the polymer. From the plots of the $\Delta G_{\text{on}}^{\ddagger}$ -values versus the polymer lengths, the differences in the energy barriers for the various threading processes are visible (Figure 5b). The lines that can be drawn through the data points have similar slopes, indicating similar sliding energies for the threading processes. Once equilibrium is achieved, it is possible to estimate the binding constants of **1** with polymers **2–4** under the different conditions studied. Table 2 shows that the affinity of macrocycles **H₂-1** and **Zn-1** for the viologen moiety changes depending on the experimental conditions. After zinc insertion, there is a decrease in the association constant owing to the abovementioned solvent competition. A similar effect is observed when py is present, although it should be noted that after removal of the axial ligands upon threading on the polymer, they will probably bind to the zinc ion on the outside of the cavity. An increased value of K_{a} is obtained in the presence of tbbpy, since this ligand eliminates the solvent competition and in addition causes a positive allosteric effect on **Zn-1**, enhancing the binding for viologens as we showed previously.¹¹ The measured values are in close accordance to the ones previously obtained for the complexation of 1,1'-dimethyl-4,4'-bipyridinium ion in the cavity of **Zn-1**.¹¹

(11) Thordarson, P.; Coumans, R. G. E.; Elemans, J.; Thomassen, P. J.; Visser, J.; Rowan, A. E.; Nolte, R. J. M. *Angew. Chem., Int. Ed.* **2004**, *43*, 4755–4759.

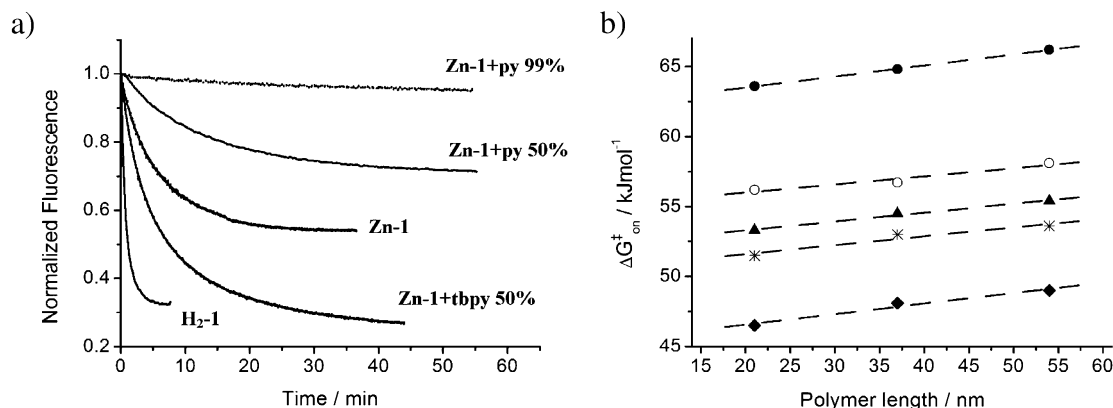


Figure 5. (a) Normalized fluorescence intensity of **H₂-1** and of **Zn-1** in the absence and presence of different ligands measured vs time after the addition of 1 equiv of polymer **2** ($[M-1] = [2] \approx 0.7 \mu\text{M}^{-1}$, $\text{CHCl}_3/\text{MeCN}$ (1/1, v/v)). (b) $\Delta G^\ddagger_{\text{on}}$ -values for the threading of **H₂-1** (◆) and **Zn-1** in the absence of ligand (▲) and in the presence of tbpy (*) or py (○ for 50% bound; ● for 99% bound) plotted vs the length of **2–4**.

Table 3. Number Averaged Molecular Weight (M_n), Degree of Polymerization (DP_n), Polymer Length (L_n) and Polydispersity Index (PDI) of Polymer Appended Viologens **2–4**

polymer	M_n (g mol ⁻¹)	DP_n	L_n (nm)	PDI
2	3140	34	21	1.03
3	5030	60	37	1.03
4	7040	88	54	1.03

Conclusion

In conclusion, we have obtained useful insight in the threading of a toroidal host on a polymer chain and its movement toward a viologen trap. Although the process is clearly dependent on the polymer length, there is now substantial evidence that the rate of threading of **Zn-1** and therefore also of our processive catalyst² can be controlled by coordination of axial ligands. In contrast to the catalytic system, which interacts with the polymer, the “cost of movement”, $70 \text{ J mol}^{-1} \text{ nm}^{-1}$, is the same for both metal and metal-free toroids. The described approach offers a novel method to study polymer mechanics, and current studies are directed at larger and more functional polymer threads.

Experimental Section

Polymer appended viologens **2–4** were synthesized according to a previously reported procedure.⁵ The properties of the polymers are summarized in Table 3.

Fluorescence experiments were performed on a Perkin-Elmer LS50B luminescent spectrometer equipped with a thermostatted cuvette holder. The excitation and emission slits were both set to 10 nm. All the experiments were done in a $\text{CHCl}_3/\text{MeCN}$ (1:1, v/v) solvent mixture.

The threading kinetics were measured using a time-drive application of the spectrometer software. Table 4 shows the wavelength at which each sample was excited and the emission wavelength that was recorded versus time.

Typically, to a weighed solution of $\sim 0.7 \mu\text{M}$ of **1**, 1 equiv of **2–4** (obtained from a $\sim 60 \mu\text{M}$ stock solution) was added and mixed. After the mixing time ($\sim 10 \text{ s}$) the measurement was started.

Determination of k_{on} . The data were analyzed by assuming that the first part of the curve is a simple second-order reaction: $A + B \rightarrow C$. All experiments were carried out with $[A] = [B]$, therefore the

Table 4. Excitation and Emission Wavelengths Used in the Different Threading Experiments Involving Macrocycles **H₂-1** and **Zn-1** and Polymers **2–4** at 296K

	H₂-1	Zn-1	Zn-1 + tbpy (50% bound)	Zn-1 + py (50% bound)	Zn-1 + py (99% bound)
$\lambda_{\text{exc}}/\text{nm}$	421	427	429	428	428
$\lambda_{\text{em}}/\text{nm}$	643	607	609	608	610

reaction becomes $2A \rightarrow C$. The integrated rate law for this reaction is $[A]^{-1} = k_{\text{on}}t$. By now plotting $[I]^{-1}$ versus time, a linear plot is obtained with the slope equal to k_{on} which is obtained via the least-squares method.

Determination of K_a . Since k_{on} is known, it can be now used to also calculate K_a by fitting the kinetic data to¹²

$$[C] = p \frac{1 - \exp(k_{\text{on}}(p - q)t)}{1 - \frac{q}{p} \exp(k_{\text{on}}(p - q)t)} \quad (1)$$

with $p = [C]_{\text{eq}}$ and $q = [A]_0[B]_0/[C]_{\text{eq}}$, where

$$[C]_{\text{eq}} = \frac{1}{2} \left([A]_0 + [B]_0 + \frac{1}{K_a} - \sqrt{([A]_0 + [B]_0 + \frac{1}{K_a})^2 - 4[A]_0[B]_0} \right)$$

Acknowledgment. The Dutch National Research School for Combination Catalysis (NRSC-C) and the Council for the Chemical Sciences of The Netherlands Organization for Scientific Research (CW-NWO) are acknowledged for financial support to J.A.A.W.E. (Veni grant), A.E.R. (Vidi grant) and R.J.M.N. (Top grant).

Supporting Information Available: Crystallographic data of **H₂-1**. This material is available free of charge via the Internet at <http://pubs.acs.org>.

JA0687141

- (12) See (a) Koppelman, S. J.; vanHoeij, M.; Vink, T.; Lankhof, H.; Schiphorst, M. E.; Damas, C.; Vlot, A. J.; Wise, R.; Bouma, B. N.; Sixma, J. J. *Blood* **1996**, 87, 2292–2300. (b) Asakawa, M.; Ashton, P. R.; Ballardini, R.; Balzani, V.; Belohradsky, M.; Gandolfi, M. T.; Kocian, O.; Prodi, L.; Raymo, F. M.; Stoddart, J. F.; Venturi, M. *J. Am. Chem. Soc.* **1997**, 119, 302–310.